

Utrecht University Repository

Title	Coordination of a Phosphine-Tethered Aminoborane to Group 10 Metals
Authors	Tiddens, MR; Kappé, BT; Smak, TJ; Lutz, M; Moret, ME
Published in	Chemistry-A European Journal
Publication Date	2024-06-06
Link	https://dspace.library.uu.nl/handle/1874/471561
Citation	Tiddens, MR, Kappé, BT, Smak, TJ, Lutz, M & Moret, ME 2024, 'Coordination of a Phosphine-Tethered Aminoborane to Group 10 Metals', Chemistry-A European Journal, vol. 30, no. 32, e202400666. https://doi.org/10.1002/chem.202400666
Versions / License	Publisher version
Rights	https://www.uu.nl/en/university-library/license-and-reuse-conditions

Coordination of a Phosphine-Tethered Aminoborane to Group 10 Metals

Martine R. Tiddens,^[a] Bram T. Kappé,^[a] Tom J. Smak,^[a] Martin Lutz,^[b] and Marc-Etienne Moret^{*[a]}

While π -complexes of C=C bonds are ubiquitous in organometallic chemistry, analogous complexes of the isoelectronic but strongly polarized B=N double bond of aminoboranes are extremely scarce. To address this gap, a diphosphine-aminoborane ligand (^{Ph}DPBA^{Pr}) is introduced and its coordination with group 10 metals is investigated. The B=N bond does not coordinate to the metal in Pt(0) and Pd(II) complexes. In contrast, side-on coordination of the B=N bond is observed in the Ni(0) complex (^{Ph}DPBA^{Pr})Ni(NCPh), and the X-ray crystal

structure reveals B–N bond elongation compared to the free ligand. The choice of co-ligand strongly influences the presence or absence of side-on coordination at Ni(0) as evidenced by NMR spectroscopy. While the B=N π -complex is geometrically similar to C=C analogues, a bonding analysis reveals that the interaction of the B=N motif with the electron-rich Ni(0) center is best described as 3c4e hyperbond, in which Ni and N are competing for the empty orbital on B.

Introduction

Transition metal complexes of π -ligands like alkenes and alkynes are pivotal intermediates in catalytic reactions including hydrogenations, hydroadditions, and polymerizations. Their coordination is generally described by the Dewar–Chatt–Duncanson (DCD) model,^[1,2] which consists of two orbital interactions: π -donation to the metal and backbonding from the metal to a ligand π^* orbital. These interactions give rise to two resonance structures: the π -complex (Figure 1, A) and the metalocycle extreme (Figure 1, B), the latter dominating with strong π -backdonation.

π -Complexes of polar double bonds are attracting interest. An electronegative heteroelement (C=N, C=O) lowers both the π and π^* orbital, resulting in primarily acceptor ligands.^[3–6] In contrast, the electron-deficient element boron affords anionic borataalkene (C=B)[−] ligands (Figure 1, C),^[7] which engage in both alkyl-like η^1 -(C) and alkene-like η^2 -(B,C) coordination.^[7–11] Bourissou and co-workers reported a platinum complex of an η^2 -(P=B) phosphineborane (Figure 1, D) exhibiting a polarized DCD bonding situation: bonding occurs mainly from phosphorus and backbonding mainly towards boron.^[12]

A perhaps more common class of compounds featuring polar π -bonds are aminoboranes (R₂BNR₂). These are intermediates in the dehydrogenation of amine boranes,^[13] and their B–N bond is described by two resonance extremes (Figure 1): one features a nitrogen-centered lone pair (E), and the other a dative N→B π -bond (F).^[14,15] Though isoelectronic to the C=C bond, the polar B=N bond differs in reactivity.^[16] Aminoborane monomers can dimerize under ambient conditions,^[17] and B=N bonds have a relatively low rotation barrier (5–25 kcal/mol).^[15,18] Since a B–N bond rotation disrupts the dative π -bond, it is associated with B–N bond elongation.^[19] Similar elongation is observed in boranes bearing more than one π -donating amino substituent due to competition for the empty orbital on boron.^[20]

Somewhat surprisingly, the coordination chemistry of isolated B=N bonds to transition metals is virtually unexplored. If B–H bonds are present, σ -(B,H) bond coordination is generally preferred.^[21–25] Calculations indicate that side-on B=N coordination is energetically less favorable, but accessible.^[21,26–28] One structurally characterized η^2 -(B=N) complex was recently prepared by Ozerov and co-workers (Figure 1, G)^[29] via N–H activation across an iridium-boryl bond. We reasoned that the *pincer* ligand design, which positions a functional group in close proximity to a metal center, would help stabilizing side-on coordination of an B=N motif. Supporting this idea, group 10 examples of related *pincer* η^2 -olefin complexes have been reported for Pd^[30] and Ni.^[31,32]

Herein, we describe the synthesis of bis[2-(diphenylphosphino)-phenyl](diisopropylamino)-borane (^{Ph}DPBA^{Pr}), a new *pincer* ligand with a B=N fragment at the central position. We investigate its coordination to group 10 metals. While the B=N bond remains uncoordinated in most cases, one Ni(0)-complex featuring the desired side-on coordination mode is isolated and structurally characterized (Figure 1, this work). Computational investigations shed light on its unusual bonding situation.

[a] M. R. Tiddens, B. T. Kappé, T. J. Smak, Dr. M.-E. Moret
Organic Chemistry and Catalysis, Faculty of Science, Utrecht University
Institute for Sustainable and Circular Chemistry
Universiteitsweg 99, 3584 CG, Utrecht, The Netherlands
E-mail: m.moret@uu.nl

[b] Dr. M. Lutz
Structural Biochemistry, Faculty of Science, Utrecht University
Bijvoet Centre for Biomolecular Research
Universiteitsweg 99, 3584 CG, Utrecht, The Netherlands

Supporting information for this article is available on the WWW under
<https://doi.org/10.1002/chem.202400666>

© 2024 The Authors. Chemistry - A European Journal published by Wiley-VCH GmbH. This is an open access article under the terms of the Creative Commons Attribution License, which permits use, distribution and reproduction in any medium, provided the original work is properly cited.

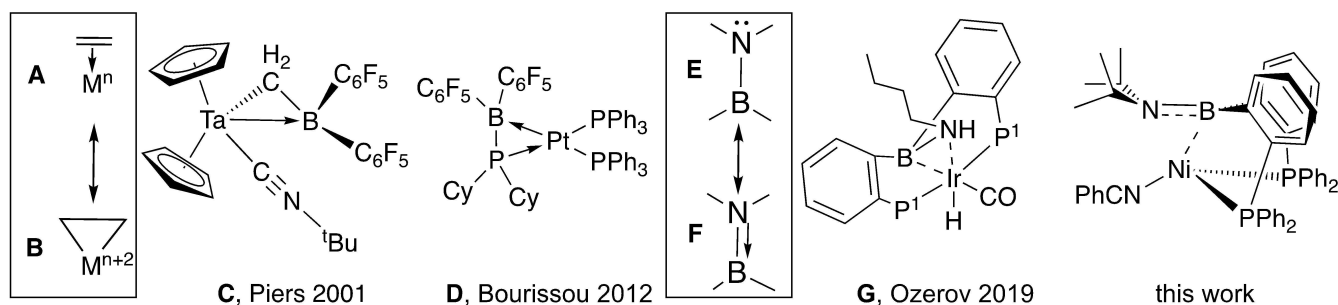


Figure 1. Schematic bonding of ethylene (A and B) to a transition metal centre; Resonance extremes of the nitrogen lone pair in aminoborane (E and F); Examples of polarized ligands coordinating to transition metal centres (C, D and G) including this work ($P^1 = P(iPr)_2$; Cy = cyclohexyl; PhCN = benzonitrile; arrows indicate dative bonds).

Results and Discussion

The $^{Ph}DPBA^{iPr}$ ligand was synthesized by reacting dichloro(diisopropylamino)borane with two equivalents of *o*-(diphenylphosphino)phenyllithium^[33,34] (Scheme 1). Its X-ray crystal structure (Figure 2) exhibits crystallographic C_2 -symmetry. A relatively short B1–N1 bond (1.396(3) Å) and a small C1–B1–N1–C19 A torsion angle ($-1.7(2)^\circ$) are consistent with a N→B π -bond.^[15,17] Furthermore, long P...B distances (3.1603(9) Å) indicate no dative interaction akin to that found for the related triphosphine-borane [*o*-(*iPr*₂P)C₆H₄]₃B (P...B = 2.154 Å).^[35]

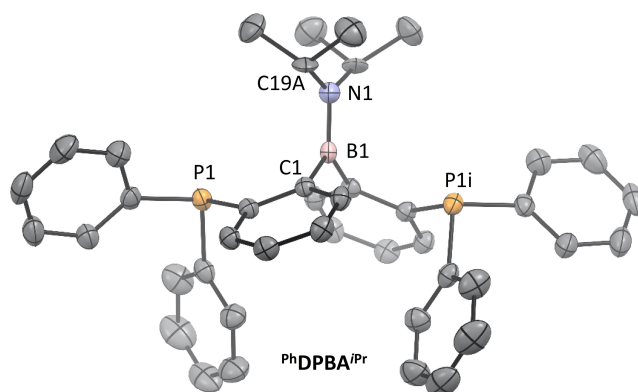
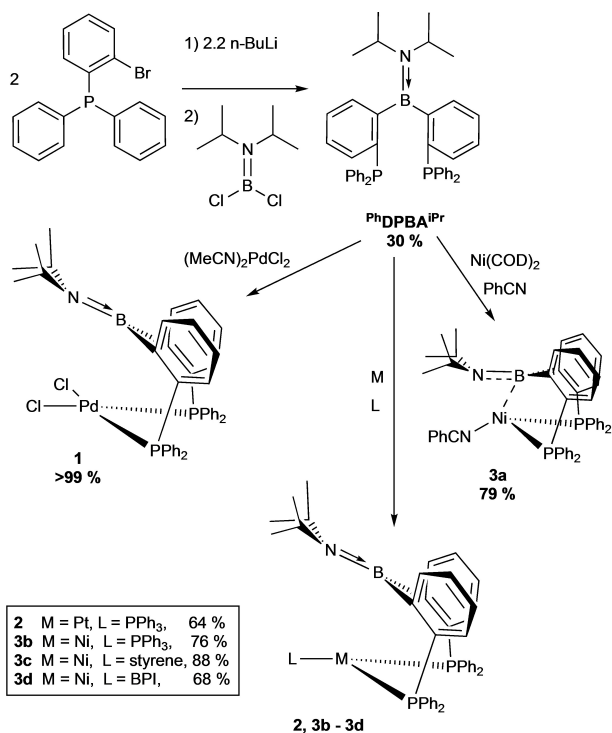


Figure 2. Molecular structure in the crystal of $^{Ph}DPBA^{iPr}$. Ellipsoids are drawn at 50% probability. Only the major conformation of the disordered isopropyl group is shown. Hydrogen atoms are omitted for clarity. Selected bond lengths (Å) and angles (deg): B1–N1 1.396(3), P1...B1 3.1603(9), C1–B1–N1–C19 A $-1.7(2)$, ΣB 360.00(19), ΣN 360.0(6). Symmetry code $i: 1/2-x, y, -z$.



Scheme 1. Synthesis of $^{Ph}DPBA^{iPr}$ in two steps (step 1: Et₂O, $-78^\circ C$ to rT, 1 h; step 2: toluene, $-78^\circ C$ to rT, overnight) and coordination of $^{Ph}DPBA^{iPr}$ to Pd(II) (1; THF, 30 min, rT), Pt(0) (2; THF, $50^\circ C$, 36 h), and Ni(0) in the presence of various co-ligands (BPI = benzophenone imine; PhCN = benzonitrile). The Ni-complexes are synthesized in overnight reactions which are performed in benzene at rT.

In solution, $^{Ph}DPBA^{iPr}$ displays a broad ^{11}B NMR signal at δ_B 44 ppm.^[17] A single ^{31}P NMR resonance (δ_P -10.1 ppm) is observed at room temperature, which decoalesces at $-90^\circ C$ into three singlets (δ_P -9.5 ppm, -14.1 ppm and -14.5 ppm) in a ratio of 2:2:3 (Figure S1). This suggests that $^{Ph}DPBA^{iPr}$ exists as a mixture of an unsymmetric and a symmetric conformer (Scheme S1) which are connected by a C–B rotation but do not feature a P→B interaction. In support of this interpretation, DFT calculations predict a small energy difference (0.8 kcal/mol) between these two conformers (see SI section 2.1). The absence of intramolecular P→B bonds, which are observed in related diphosphine-borane compounds,^[35–37] likely originates from π -donation from the nitrogen substituent decreasing the Lewis acidity of the borane.

Treating $^{Ph}DPBA^{iPr}$ with (MeCN)₂PdCl₂ afforded the yellow complex ($^{Ph}DPBA^{iPr}$)Pd(II)Cl₂ (1) quantitatively (Scheme 1). An X-ray crystal structure determination (Figure 3) revealed a square planar geometry ($\Sigma Pd = 360.28(3)^\circ$) with the two chloride ligands in *cis*-positions. The $^{Ph}DPBA^{iPr}$ ligand coordinates overall $\kappa^2(P,P)$ with a P–Pd–P angle of $94.771(16)^\circ$ and a small C62–C12–C11–C61 torsion angle of $-23.4(2)^\circ$. This torsion angle is smaller than that in analogous Pd(II) complexes of PEP-pincer ligands (E=CH₂: 40° ,^[38] E=S: 30° ^[39]), which suggests

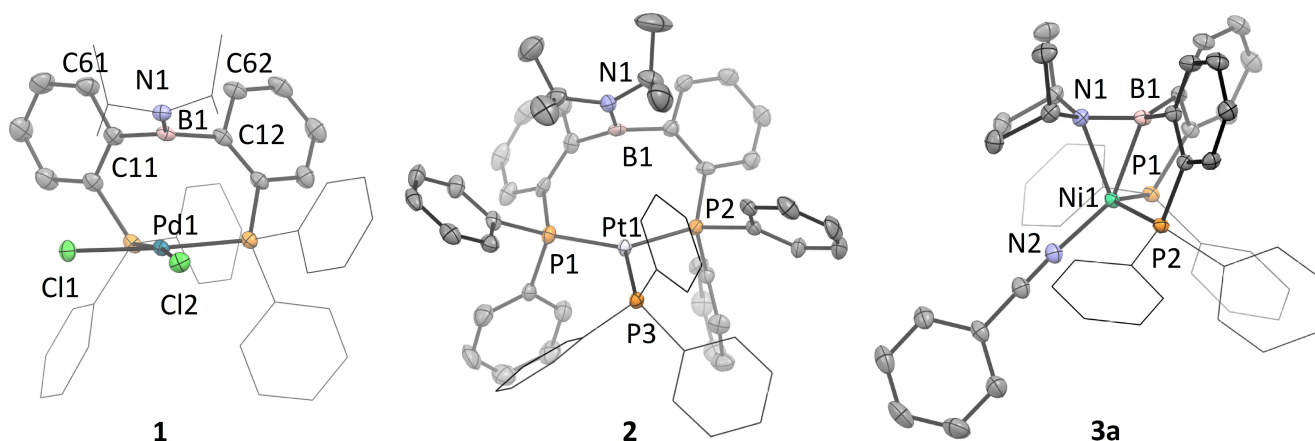


Figure 3. Molecular structures in the crystals of **1**, **2** and **3a**. Ellipsoids are drawn at 50% probability. For clarity, hydrogen atoms are omitted and selected phenyl-rings are displaced in wireframe style (as well as the isopropyl-residues in **1**). Selected bond lengths (Å) and angles (deg), for complex **1**: B1–N1 1.404(2), Pd...B1 2.903(2), Pd...N 3.3884(15), C61–C11–C12–C62 23.39, P1–Pd1–P2 94.771(16), Σ B 357.0(3), Σ N 359.8(3). For complex **2**: B1–N1 1.405(9), Pt1...B1 3.368(8), Pt1...N1 3.868(5), P1–Pt1–P2 121.03(7), Σ B 355.5(11), Σ N 359.9(10). For complex **3a**: B1–N1 1.4940(18), Ni1–B1 2.1397(15), Ni1–N1 2.1438(11), P1–Ni1–P2 119.357(15), Σ B 354.30(19), Σ N1 353.32(18).

that a central boron atom renders the ligand backbone somewhat more flexible than a carbon or sulfur atom.

The aminoborane unit is not coordinated to the Pd(II)-center, as shown by Pd...B (2.903(2) Å) and Pd...N (3.3884(15) Å) distances being significantly longer than the sum of covalent radii (Pd,B: 2.23 Å; Pd,N: 2.1 Å).^[40] Even though these distances are within the sum of van der Waals radii (Pd,B: 4.06 Å; Pd,N: 3.81 Å),^[41] which might suggest a weak interaction, the position of the B–N bond is more likely imposed by the rigid backbone of the κ^2 (P,P) $\text{PhDPBA}^{\text{Pr}}$ ligand. Supporting this interpretation, the boron atom is only slightly pyramidalized (Σ B = 357.0(3)°), the nitrogen atom remains planar (Σ N = 360.0(6)°), and the B–N bond is not elongated compared to the free ligand.

In the solid state, the B=N motif is roughly parallel to the Pd–Cl2 bond (Figure 3), rendering the two phosphorus atoms chemically inequivalent. In solution, a single ^{31}P NMR signal at δ_{p} 36.1 ppm suggests the presence of a fast, fluxional process involving a pendulum motion of the B=N fragment from Cl1 to Cl2 facilitated by the flexible 8-membered chelate ring. Tauchert and co-workers observed a similar fluxional process for $\text{PhDPB}^{\text{Ph}}\text{–PdCl}_2$ (PhDPB^{Ph} = bis[2-(diphenylphosphino)phenyl]borane) featuring a pendular B–C_{ph} motif.^[42] In that case, the η^1 -(B) coordination of the B–C_{ph} to Pd(II) decreases the flexibility of the ligand backbone resulting in a broad ^{31}P NMR signal at room temperature which splits into two broad singlets at –30 °C.

The bidentate coordination mode of $\text{PhDPBA}^{\text{Pr}}$ in **1** also contrasts with the tridentate coordination of PrDPB^{Ph} to Pd(II),^[43] for which a weak Pd→B interaction is observed (Pd–B: 2.650(3) Å, Σ B = 354.9(9)°). This difference is in line with the nitrogen-centered lone pair being much more π -donating to the formally empty orbital on boron than a phenyl group, making the borane less σ -accepting.

Next, coordination to a more basic Pt(0)-center was investigated. Heating a 1:1 mixture of $\text{PhDPBA}^{\text{Pr}}$ and Pt(PPh₃)₄ in THF for 36 h at 50 °C afforded complex ($\text{PhDPBA}^{\text{Pr}}$)Pt(0)PPh₃ (**2**) in 64% yield (Scheme 1). The ^{31}P NMR spectrum of **2** is

consistent with an A₂B system^[44] with $^2J_{\text{A,B}}$ = 125 Hz, and its 8-lines ^{195}Pt NMR spectrum can be simulated as an A₂BX system^[45] (X=Pt) with $^1J_{\text{A,X}}$ = 4521 Hz, $^1J_{\text{B,X}}$ = 4231 Hz and $^2J_{\text{A,B}}$ = 125 Hz. Both spectra indicate that the two phosphorus atoms of the $\text{PhDPBA}^{\text{Pr}}$ ligand are equivalent in **2**. In the ^{13}C NMR spectrum of **2**, the B–C (δ_{c} 154.5 ppm) and N–C (δ_{c} 50.3 ppm) signals have very similar chemical shifts to those of free $\text{PhDPBA}^{\text{Pr}}$ (δ_{c} 154.7 ppm; δ_{c} 50.6 ppm) and complex **1** (δ_{c} 153.0 ppm; δ_{c} 54.2), suggesting that the B=N motif does not coordinate to the Pt(0)-center.

This was confirmed by an X-ray crystal structure determination (Figure 3). The platinum center adopts a slightly distorted trigonal geometry with κ^2 (P,P) coordination of $\text{PhDPBA}^{\text{Pr}}$ and one additional PPh₃ ligand. The P–Pt–P bite angle of $\text{PhDPBA}^{\text{Pr}}$ (121.03(7)°) is significantly larger than in the square planar Pd(II) complex **2**. As suggested by the spectroscopic data, the B=N motif does not coordinate to Pt: the Pt...B (3.368(8) Å) and Pt...N distance (3.868(5) Å) are significantly longer than the sum of covalent radii (Pt,B 2.2 Å and Pt,N 2.07 Å).^[40] The boron atom is slightly pyramidalized (Σ B = 355.5(11)°), but much less than observed for phosphine-tethered Pt(0)→B retrodonative bonds (Σ B = 334°–336°)^[37,46] or related η^2 -(B,C_{ph})^[37] and η^2 -(P=B)^[12] complexes (Σ B = 345°–354°). The slight pyramidalization in **2** likely originates from strain imposed by the $\text{PhDPBA}^{\text{Pr}}$ bite angle rather than from a direct Pt...B interaction. A space-filling model of **2** (Figure S4) illustrates how the isopropyl substituents on nitrogen and the PPh₃ co-ligand compete for the same space, suggesting that steric repulsion may prevent B=N motif coordination. Our combined observations on **1** and **2** show that $\text{PhDPBA}^{\text{Pr}}$ can accommodate a wide range of P–M–P bite angles (94°–121°) which is tentatively ascribed to the flexibility of the central boron atom.

Finally, nickel(0) was found to be the metal of choice to access the desired η^2 -(B,N) coordination mode, combining relatively strong basicity with facile ligand exchange. Treating $\text{PhDPBA}^{\text{Pr}}$ with Ni(COD)₂ and benzonitrile afforded the nickel

complex **3a** in 79% yield (Scheme 1). Its X-ray crystal structure (Figure 3) reveals a distorted tetrahedral geometry with $\kappa^2(\text{P},\text{B}=\text{N},\text{P})$ coordination of $\text{PhDPBA}^{\text{IPr}}$, the aminoborane fragment engaging in $\eta^2\text{-(B,N)}$ coordination to Ni(0). The Ni–B and Ni–N distances are comparable (Ni–B: 2.1397(15) Å and Ni–N: 2.1438(11) Å), resulting in a symmetric coordination geometry. A substantial B–N bond elongation (1.4940(18) Å vs 1.396(3) Å in $\text{PhDPBA}^{\text{IPr}}$) and pyramidalization of both B and N atoms ($\Sigma\text{N} = 353.32(18)^\circ$, $\Sigma\text{B} = 354.30(19)^\circ$) closely match the geometrical changes observed for olefins upon coordination.

The similar Ni–B and Ni–N bond lengths contrast with the $(\text{IPr})\text{PB}^{\text{N(H)NBuPr}}\text{Ir(H)CO}$ complex (Figure 1, G),^[29] to our knowledge the only other structurally characterized $\eta^2\text{-(B,N)}$ coordination of an aminoborane unit. There, the longer Ir–B distance (2.272(3) Å) compared to Ir–N (2.175(2) Å) have been interpreted as a retrodative B←Ir bond complemented by a dative N→Ir bond. The more symmetrical B=N coordination in **3a** suggests a stronger accepting character of the B=N fragment when bound to Ni(0) as compared to the less electron-rich Ir(I).

Spectroscopic evidence for $\eta^2\text{-(B,N)}$ coordination in solution was obtained by NMR. A single ^{31}P NMR signal at 25 ppm indicates a symmetric coordination of $\text{PhDPBA}^{\text{IPr}}$ to nickel, and the upfield shift of the ^{11}B NMR signal of **3a** to $\delta_{\text{B}} 23$ ppm ($\Delta\delta_{\text{B}} = -20$ ppm compared to free $\text{PhDPBA}^{\text{IPr}}$) supports borane coordination.^[47] Furthermore, shifted B–C ($\delta_{\text{C}} 161$ ppm, $\Delta\delta_{\text{C}} = +6$ ppm) and N–C ($\delta_{\text{C}} 58$ ppm, $\Delta\delta_{\text{C}} = +7$ ppm) ^{13}C NMR signals with respect to free $\text{PhDPBA}^{\text{IPr}}$ (B–C: 154.7 ppm; N–C: 50.6 ppm) confirm symmetric side-on coordination of the B=N bond in solution. These ^{13}C NMR signals are convenient handles complementary to ^{11}B NMR in assessing side-on B=N coordination in solution (Table S2).

To investigate co-ligand effects on B=N coordination, Ni(0)-complexes of $\text{PhDPBA}^{\text{IPr}}$ featuring either PPh_3 (**3b**), styrene (**3c**) or benzophenone imine (BPI, **3d**) as stabilizing co-ligand were synthesized following similar procedures (Scheme 1). The ^{31}P NMR spectrum of $(\text{PhDPBA}^{\text{IPr}})\text{Ni(0)PPh}_3$ (**3b**) displays an A_2B system ($^2J_{\text{A,B}} = 79$ Hz) consistent with a $\kappa^2(\text{P},\text{P})$ coordination of $\text{PhDPBA}^{\text{IPr}}$ to the Ni(0)-center, which is additionally stabilized by a PPh_3 co-ligand. Furthermore, the characteristic ^{13}C NMR and ^{11}B NMR handles (Table S2) indicate a pendant B=N motif, making **3b** isostructural to **2**. Next to PPh_3 , a competing π -ligand (styrene) or a larger co-ligand (BPI) can also displace the $\eta^2\text{-(B,N)}$ coordination as inferred from the ^{13}C and ^{11}B NMR spectra of **3c** and **3d**, respectively (see SI for full NMR analysis). Of note, a close inspection of multinuclear NMR data for **3d** suggests a rapid equilibrium between two isomers, coordination of the B=N bond being coupled with a change of coordination mode of the BPI ligand from $\eta^2\text{-(C=N)}$ to $\eta^1\text{-(N)}$ (see SI section 2.4). Hence, the B=N interaction can be displaced by either a donor ligand (PPh_3) or a π -acceptor ligand (styrene). This contrasts with analogous nickel complexes featuring a side-on coordinated ketone, which is only displaced by a strongly π -accepting alkyne but not by PPh_3 or styrene.^[3] This difference likely has both steric and electronic origins: the isopropyl substituents on N clash with large ligands such as PPh_3 , while the $\eta^2\text{-(B,N)}$ coordination is weaker than $\eta^2\text{-(C,O)}$ coordination allowing its facile displacement by π -ligands.

Consequently, only a small donor ligand such as $\eta^1\text{-PhCN}$ allows for the targeted $\eta^2\text{-(B,N)}$ coordination.

The frontier Kohn–Sham molecular orbitals of **3a** feature five filled orbitals of primarily d-character, which supports a d^{10} configuration (Figure S42). One of them (HOMO–1) shows some bonding with boron. More insights into the nature of the interaction of the B=N motif with Ni(0) in **3a** is provided by DFT calculations including Natural Bond Orbital (NBO)^[48] and Quantum Theory of Atoms in Molecules (QTAIM)^[49,50] analysis.

NBO analysis of the free ligand $\text{PhDPBA}^{\text{IPr}}$ identifies a strongly polarized $\sigma\text{-(B,N)}$ bonding orbital (19% B; 81% N) and an N-centered lone pair with 99% p character in the principal Lewis structure (similar to resonance structure E in Figure 1). Second order perturbation analysis finds a strong donation (76.7 kcal/mol) from the N lone pair to an empty B-centered p orbital. Significant $\pi\text{-(B,N)}$ bonding is additionally confirmed by a B–N Wiberg bond index (WBI) of 1.04 (see SI section 5.3). As a consequence, the natural localized molecular orbital (NLMO) derived from the N lone pair is strongly delocalized towards B (14%, Figure S40). Reassuringly, imposing the Lewis structure containing a B=N double bond as a starting point yields a very similar NLMO, now derived from the $\pi\text{-(B,N)}$ bonding orbital. N contributions of 76%–85% for the σ - and $\pi\text{-(B,N)}$ bonds have been previously reported and attributed to the formal dative character of the B–N π bond.^[51]

Upon coordination of the B=N π -bond to nickel (**3a**), the total natural charge of the BN fragment decreases by $\Delta q(\text{B}=\text{N}) = -0.34 e^-$, indicating transfer of electron density from nickel to the acceptor B=N motif (Table S5). The charge on nitrogen remains almost constant ($\Delta q(\text{N}) = -0.02 e^-$) while the charge on boron changes significantly ($\Delta q(\text{B}) = -0.32 e^-$), suggesting that most of the bonding occurs between Ni and B. WBIs of 0.32 for the (Ni,B) atom pair and of only 0.10 for (Ni,N) confirm the electronically unsymmetric nature of the Ni–(BN) interaction.

This dissymmetry is supported by a QTAIM analysis of the electron density in **3a** (Figure S41). It identifies a Ni–B bond critical point (BCP) in the negative Laplacian region ($\nabla^2\rho = -0.15$ a.u.), indicative of a covalent interaction. In contrast, the Ni–N BCP ($\nabla^2\rho = +0.084$ a.u.) is found very close to the corresponding ring critical point (RCP), implying that the BCP is a very shallow density maximum on the interatomic surface, consistent with a very weak, ionic Ni–N interaction. In stark contrast, a previously reported QTAIM analysis on a closely related $\eta^2\text{-olefin}$ complex of Ni(0)^[31] shows ionic Ni–C bonds and a central RCP, both consistent with electronically symmetric bonding of the olefin motif to nickel.

A more detailed bonding picture is again provided by an NBO analysis of **3a**, which finds a principal Lewis structure featuring five filled, nonbonding d orbitals on the Ni(0) center and a lone pair on N (Figure 4, top box). Consequently, the B–N interaction is described as a single bond. Second order perturbation analysis identifies Ni→B (14.3 kcal/mol) and N→B (59.3 kcal/mol) donations. The latter is significantly weaker than the N→B donation in the $\text{PhDPBA}^{\text{IPr}}$ ligand (*vide supra*), which suggests that nitrogen and nickel act as competing donors to an empty orbital on B. In support of this idea, the NLMOs (Figure 4, top) derived from the 5th d orbital on nickel and from

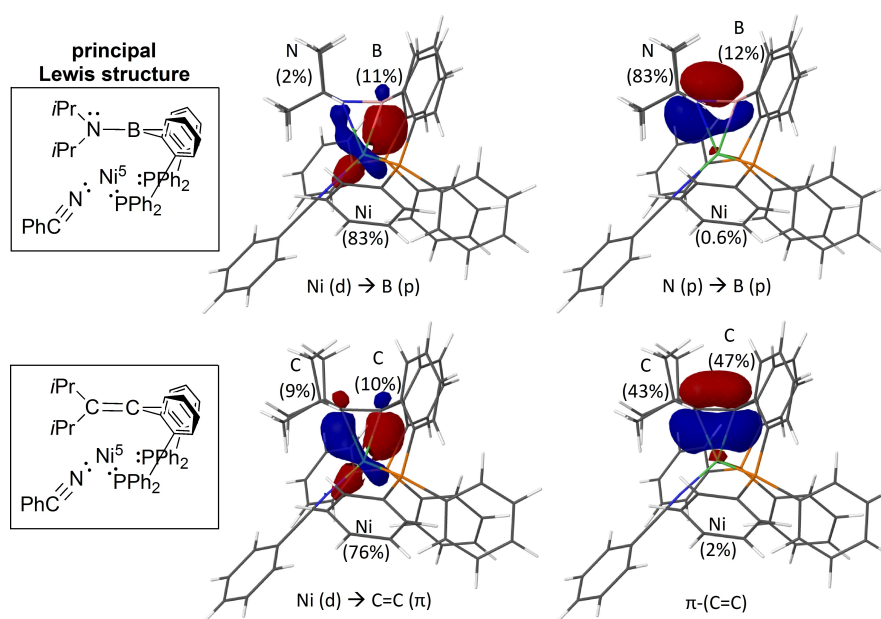
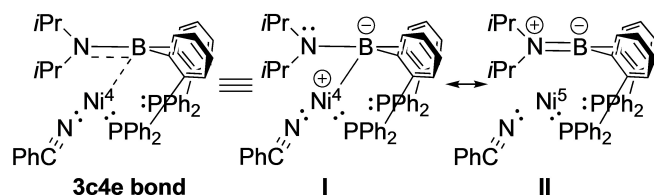


Figure 4. Left: Principal Lewis structure of **3a** (top) and of a hypothetical **(olefin)-Ni-PhCN** complex (bottom); the number on Ni refers to the number of filled d orbitals. Right: selected NLMOs derived from one d orbital on nickel and either from the N-centered lone pair of **3a** (top) or from the olefin π -bonding orbital (bottom). Atomic contributions (%) are reported in parentheses. Heteroatoms are coloured green for Ni, blue for N, pink for B and orange for P (see SI for details on Computational methods).

the N-centered lone pair both have substantial delocalization tails to B (11–12%). In contrast, the energy for $N \rightarrow Ni$ donation is much smaller (2 kcal/mol), and the corresponding NLMO (Figure 4, top right) only has 0.6% Ni character, confirming a weak orbital interaction between Ni and N. To be complete, some level of N,Ni interaction is indirectly accounted for by a donation of the $\sigma(B,N)$ bond to the vacant $Ni(4s)$ orbital (12.3 kcal/mol).

From this analysis emerges a description of the bonding situation in the N,B,Ni-triad as primarily consisting of a 3c4e hyperbond. It is a superposition of two resonance structures (I and II in Scheme 2) in which the central element (B in this case) is bonded to one of the terminal elements (N or Ni) while the other one hosts a lone pair. In support of this interpretation, either of the two Lewis structures I and II were assigned a lower non-Lewis percentage than the principal Lewis structure when imposed to the NBO procedure, suggesting that they are at least as good representations of the total electron density. In both calculations, the NBO procedure found evidence for 3c4e bonding with an approximate 50/50 contribution of I and II. Related 3c4e bonding has been proposed for the N,B,N triad in $HB(NH_2)_2$.^[52] Also, B–N bond elongation in a series of $(NH_2)_xBH_{3-x}$



Scheme 2. Resonance structures of **3a** (the number on Ni refers to the number of filled d orbitals).

compounds has been attributed to reduced π -bonding due to π -donors competing for the empty orbital on B.^[53] The elongation of the B–N bond upon binding to Ni in **3a** can be similarly accounted for by the Ni center competing with the N-centered lone pair for the empty orbital on boron.

This bonding picture can be compared to the coordination of a polarized P=B bond to Pt(0) (Figure 1, D).^[12] There, significant P→Pt bonding significantly contributes to the side-on P=B coordination. In contrast, N–Ni orbital interactions are weak in compound **3a**. More generally, a more covalent bonding picture is observed in structure D than in **3a**, which is imputable to small electronegativity differences between the involved atoms (P 2.2; Pt 2.2 and B 2.0) as compared to **3a** (Ni 1.9; N 3.0).^[54] In addition, it is of interest to compare the donor-acceptor interactions (second order perturbation analysis) derived from Lewis structure II to those in an analogous (η^2 -olefin)-Ni-PhCN complex (Figure 4, bottom). The energy associated to π backdonation ($Ni(d) \rightarrow \pi^*(C=C)$: 53 kcal/mol) is significantly larger than that in **3a** ($Ni(d) \rightarrow \pi^*(B=N)$: 21 kcal/mol). The π -donation in both systems is closer in energy ($\pi(C=C) \rightarrow Ni(s)$: 20 kcal/mol; $\pi(B=N) \rightarrow Ni(s)$: 15 kcal/mol). The stronger π -accepting ability of the C=C BH bond compared to the isoelectronic B=N bond can be explained by a symmetry mismatch between donor orbital $Ni(d)$ and acceptor orbital $\pi^*(B=N)$, the latter having a large coefficient on B (see Figure 4, bottom for NLMOs). The weakly accepting character of the B=N motif also explains the propensity of $PhDPBA^{iPr}$ to adopt a $\kappa^2(P,P)$ binding mode even though the ligand positions the motif in close proximity to electron-rich transition metal centers (*vide supra*).

Conclusions

In conclusion, incorporation of an aminoborane fragment into a pincer ligand enabled the study of η^2 -(B,N) coordination to Ni(0). Spectroscopic and crystallographic data provides evidence for a symmetric coordination and B–N bond elongation. While these observations are commonly associated with olefin side-on coordination, computational bonding analysis supports a distinct description as a 3c4e hyperbond for the Ni,B,N triad. Compared to an olefin analogue, the bonding of the BN fragment to the metal is tenuous, and therefore the motif is easily displaced. The resulting flexible κ^2 (P,P) coordination mode of $\text{P}^{\text{h}}\text{DPBA}^{\text{Pr}}$ is more readily accessible and was observed in Pd(II)- and Pt(0) complexes with different bite angles. In the broader context of metal-ligand cooperation, the B=N fragment is envisioned to function as a hemilabile motif. Consequences for small molecule activation are currently under investigation in our group.

Supporting Information

Deposition Numbers 2303012-2303015 contain the supplementary crystallographic data for this paper. These data are provided free of charge by the joint Cambridge Crystallographic Data Centre and Fachinformationszentrum Karlsruhe Access Structures service.

The authors have cited additional references within the Supporting Information.^[55–65]

Acknowledgements

This project has received funding from the European Research Council (ERC) under the European Union's Horizon 2020 research and innovation program (grant agreement No 715060). The X-ray diffractometer has been financed by the Netherlands Organization for Scientific Research (NWO). This work made use of the Dutch national e-infrastructure with the support of the SURF Cooperative using grant no. EINF-3520. We thank Dr. Johann Jastrzebski for assistance with NMR analysis.

Conflict of Interests

The authors declare no conflict of interest.

Data Availability Statement

The data that support the findings of this study are available in the supplementary material of this article.

Keywords: Acceptor ligands · aminoboranes · group 10 metals · π -ligands · Bonding Analysis

- [1] J. Chatt, L. A. Duncanson, *J Chem Soc (Resumed)* **1953**, 2939.
- [2] D. M. P. Mingos, *J. Organomet. Chem.* **2001**, *635*, 1–8.
- [3] A. F. Orsino, M. Gutiérrez del Campo, M. Lutz, M.-E. Moret, *ACS Catal.* **2019**, *9*, 2458–2481.
- [4] D. G. A. Verhoeven, H. A. Negenman, A. F. Orsino, M. Lutz, M.-E. Moret, *Inorg. Chem.* **2018**, *57*, 10846–10856.
- [5] B. W. H. Saes, D. G. A. Verhoeven, M. Lutz, R. J. M. Klein Gebbink, M.-E. Moret, *Organometallics* **2015**, *34*, 2710–2713.
- [6] T. T. Tsou, J. C. Huffman, J. K. Kochi, *Inorg. Chem.* **1979**, *18*, 2311–2317.
- [7] K. S. Cook, W. E. Piers, T. K. Woo, R. McDonald, *Organometallics* **2001**, *20*, 3927–3937.
- [8] D. J. H. Emslie, B. E. Cowie, K. B. Kolpin, *Dalton Trans.* **2012**, *41*, 1101–1117.
- [9] R. J. Maza, J. J. Carbó, E. Fernández, *Adv. Synth. Catal.* **2021**, *363*, 2274–2289.
- [10] K. Watanabe, A. Ueno, X. Tao, K. Škoch, X. Jie, S. Vagin, B. Rieger, C. G. Daniliuc, M. C. Letzel, G. Kehr, G. Erker, *Chem. Sci.* **2020**, *11*, 7349–7355.
- [11] N. A. Phillips, R. Y. Kong, A. J. P. White, M. R. Crimmin, *Angew. Chem. Int. Ed.* **2021**, *60*, 12013–12019.
- [12] A. Amgoune, S. Ladeira, K. Miqueu, D. Bourissou, *J. Am. Chem. Soc.* **2012**, *134*, 6560–6563.
- [13] A. L. Colebatch, A. S. Weller, *Chem. Eur. J.* **2019**, *25*, 1379–1390.
- [14] Y. Mo, S. D. Peyerimhoff, *Theor. Chem. Acc.* **1999**, *101*, 311–318.
- [15] A. Haaland, *Angew. Chem. Int. Ed.* **1989**, *28*, 992–1007.
- [16] H. Hirao, H. Fujimoto, *J. Phys. Chem. A* **2000**, *104*, 6649–6655.
- [17] R. Borthakur, V. Chandrasekhar, *Coord. Chem. Rev.* **2021**, *429*, 213647–213678.
- [18] P. A. Barfield, M. F. Lappert, J. Lee, *Trans. Faraday Soc.* **1968**, *64*, 2571–2578.
- [19] D. J. Grant, D. A. Dixon, *J. Phys. Chem. A* **2006**, *110*, 12955–12962.
- [20] B. L. Kormos, C. J. Cramer, *Inorg. Chem.* **2003**, *42*, 6691–6700.
- [21] G. Alcaraz, L. Vendier, E. Clot, S. Sabo-Etienne, *Angew. Chem. Int. Ed.* **2010**, *49*, 918–920.
- [22] G. Alcaraz, S. Sabo-Etienne, *Angew. Chem. Int. Ed.* **2010**, *49*, 7170–7179.
- [23] M. C. MacInnis, R. McDonald, M. J. Ferguson, S. Tobisch, L. Turculet, *J. Am. Chem. Soc.* **2011**, *133*, 13622–13633.
- [24] T. M. Douglas, A. B. Chaplin, A. S. Weller, X. Yang, M. B. Hall, *J. Am. Chem. Soc.* **2009**, *131*, 15440–15456.
- [25] A. Kumar, N. A. Beattie, S. D. Pike, S. A. Macgregor, A. S. Weller, *Angew. Chem. Int. Ed.* **2016**, *55*, 6651–6656.
- [26] Y. Kawano, M. Uruichi, M. Shimoi, S. Taki, T. Kawaguchi, T. Kakizawa, H. Ogino, *J. Am. Chem. Soc.* **2009**, *131*, 14946–14957.
- [27] P. M. Zimmerman, A. Paul, C. B. Musgrave, *Inorg. Chem.* **2009**, *48*, 5418–5433.
- [28] P. M. Zimmerman, A. Paul, Z. Zhang, C. B. Musgrave, *Angew. Chem. Int. Ed.* **2009**, *48*, 2201–2205.
- [29] Y. Cao, W.-C. Shih, O. V. Ozerov, *Organometallics* **2019**, *38*, 4076–4081.
- [30] C. C. Comanescu, M. Vyushkova, V. M. Iluc, *Chem. Sci.* **2015**, *6*, 4570–4579.
- [31] M. L. G. Sansores-Paredes, M. Lutz, M.-E. Moret, *Nat. Chem.* **2024**, *16*, 417–425.
- [32] M. L. G. Sansores-Paredes, S. van der Voort, M. Lutz, M.-E. Moret, *Angew. Chem. Int. Ed.* **2021**, *60*, 26518–26522.
- [33] S. Harder, L. Brandsma, J. A. Kanters, A. Duisenberg, J. H. van Lenthe, *J. Organomet. Chem.* **1991**, *420*, 143–154.
- [34] F. Zhang, L. Wang, S.-H. Chang, K.-L. Huang, Y. Chi, W.-Y. Hung, C.-M. Chen, G.-H. Lee, P.-T. Chou, *Dalton Trans.* **2013**, *42*, 7111–7119.
- [35] S. Bontemps, G. Bouhadir, P. W. Dyer, K. Miqueu, D. Bourissou, *Inorg. Chem.* **2007**, *46*, 5149–5151.
- [36] B. Wang, C. S. G. Seo, C. Zhang, J. Chu, N. K. Szymczak, *J. Am. Chem. Soc.* **2022**, *144*, 15793–15802.
- [37] B. E. Cowie, D. J. H. Emslie, *Chem. Eur. J.* **2014**, *20*, 16899–16912.
- [38] W. Lesueur, E. Solari, C. Floriani, A. Chiesi-Villa, C. Rizzoli, *Inorg. Chem.* **1997**, *36*, 3354–3362.
- [39] N. Morohashi, Y. Akahira, S. Tanaka, K. Nishiyama, T. Kajiwara, T. Hattori, *Chem. Lett.* **2008**, *37*, 418–419.
- [40] B. Cordero, V. Gómez, A. E. Platero-Prats, M. Revés, J. Echeverría, E. Cremades, F. Barragán, S. Alvarez, *Dalton Trans.* **2008**, 2832.
- [41] S. Alvarez, *Dalton Trans.* **2013**, *42*, 8617.
- [42] F. Ritter, L. John, T. Schindler, J. P. Schroers, S. Teeuwen, M. E. Tauchert, *Chem. Eur. J.* **2020**, *26*, 13436–13444.
- [43] S. Bontemps, M. Sircoglou, G. Bouhadir, H. Puschmann, J. A. K. Howard, P. W. Dyer, K. Miqueu, D. Bourissou, *Chem. Eur. J.* **2008**, *14*, 731–740.
- [44] H. Friebolin, *Basic One- and Two-Dimensional NMR Spectroscopy*, Weinheim: WILEY-VCH, **2011**.

- [45] T. W. Dingle, K. R. Dixon, *Inorg. Chem.* **1974**, *13*, 846–851.
- [46] S. Bontemps, G. Bouhadir, W. Gu, M. Mercy, C.-H. Chen, B. M. Foxman, L. Maron, O. V. Ozerov, D. Bourissou, *Angew. Chem. Int. Ed.* **2008**, *47*, 1481–1484.
- [47] G. Bouhadir, D. Bourissou, in *The Chemical Bond III: 100 Years Old and Getting Stronger* (Ed.: D. M. P. Mingos), Springer International Publishing, Cham, **2017**, pp. 141–201.
- [48] All NBO analysis were performed with NBO 6.0: E. D. Glendening, J. K. Badenhoop, A. E. Reed, J. E. Carpenter, J. A. Bohmann, C. M. Morales, C. R. Landis, F. Weinhold. NBO 6.0; Theoretical Chemistry institute, University of Wisconsin: Madison, WI, **2013**.
- [49] T. Lu, F. Chen, *J. Comput. Chem.* **2012**, *33*, 580–592.
- [50] R. F. W. Bader, *Chem. Rev.* **1991**, *91*, 893–928.
- [51] G. Mierzwa, A. J. Gordon, S. Berski, *J. Mol. Model.* **2020**, *26*, 136.
- [52] K.-A. Østby, A. Haaland, G. Gundersen, H. Nöth, *Organometallics* **2005**, *24*, 5318–5328.
- [53] K.-A. Østby, T. Fjeldberg, G. Gundersen, *J. Mol. Struct.* **2001**, *567* (568), 247–268.
- [54] M. Bochmann, *Organometallics and Catalysis: An Introduction.*, Oxford University Press, USA, **2015**.
- [55] A. L. Iglesias, M. Muñoz-Hernández, J. J. García, *J. Organomet. Chem.* **2007**, *692*, 3498–3507.
- [56] A. M. M. Schreurs, X. Xian, L. M. J. Kroon-Batenburg, *J. Appl. Crystallogr.* **2010**, *43*, 70–82.
- [57] L. Krause, R. Herbst-Irmer, G. M. Sheldrick, D. Stalke, *J. Appl. Crystallogr.* **2015**, *48*, 3–10.
- [58] G. M. Sheldrick, *Acta Crystallogr A Found Adv* **2015**, *71*, 3–8.
- [59] G. M. Sheldrick, *Acta Crystallogr C Struct Chem* **2015**, *71*, 3–8.
- [60] A. L. Spek, *Acta Crystallogr. Sect. D* **2009**, *65*, 148–155.
- [61] All calculations were performed with Gaussian 16; Revision C.01, J. M. Frisch, G. W. Trucks, H. B. Schlegel, G. E. Scuseria, M. A. Robb, J. R. Cheeseman, G. Scalmani, V. Barone, G. A. Petersson, H. Nakatsuji, X. Li, M. Caricato, A. V. Marenich, J. Bloino, B. G. Janesko, R. Gomperts, B. Mennucci, H. P. Hratchian, J. V. Ortiz, A. F. Izmaylov, J. L. Sonnenberg, D. Williams-Young, F. Ding, F. Lipparini, F. Egidi, J. Goings, B. Peng, A. Petrone, T. Henderson, D. Ranasinghe, V. G. Zakrzewski, J. Gao, N. Rega, G. Zheng, W. Liang, M. Hada, M. Ehara, K. Toyota, R. Fukuda, J. Hasegawa, M. Ishida, T. Nakajima, Y. Honda, O. Kitao, H. Nakai, T. Vreven, K. Throssell, J. A. Montgomery Jr., J. E. Peralta, F. Ogliaro, M. J. Bearpark, J. J. Heyd, E. N. Brothers, K. N. Kudin, V. N. Staroverov, T. A. Keith, R. Kobayashi, J. Normand, K. Raghavachari, A. P. Rendell, J. C. Burant, S. S. Iyengar, J. Tomasi, M. Cossi, J. M. Millam, M. Klene, C. Adamo, R. Cammi, J. W. Ochterski, R. L. Martin, K. Morokuma, O. Farkas, J. B. Foresman, D. J. Fox. Gaussian 16, Revision C.01; Gaussian, Inc.: Wallingford, CT, **2016**.
- [62] S. Grimme, S. Ehrlich, L. Goerigk, *J. Comput. Chem.* **2011**, *32*, 1456–1465.
- [63] M. W. Drover, E. G. Bowes, L. L. Schafer, J. A. Love, A. S. Weller, *Chem. Eur. J.* **2016**, *22*, 6793–6797.
- [64] C. Chiu, F. P. Gabbaï, *Angew. Chem. Int. Ed.* **2007**, *46*, 6878–6881.
- [65] A. C. Malcolm, K. J. Sabourin, R. McDonald, M. J. Ferguson, E. Rivard, *Inorg. Chem.* **2012**, *51*, 12905–12916.

Manuscript received: February 19, 2024
Accepted manuscript online: April 5, 2024
Version of record online: May 8, 2024